Gravity dual and CERN LHC study of single-sector supersymmetry breaking

Maxime Gabella,[1,2,*] Tony Gherghetta,[2,†] and Joel Giedt[3,‡]

[1]*ITP, École Polytechnique Fédérale de Lausanne, CH-1015 Lausanne, Switzerland*
[2]*School of Physics and Astronomy, University of Minnesota, Minneapolis, Minnesota 55455, USA*
[3]*William I. Fine Theoretical Physics Institute, University of Minnesota, Minneapolis, Minnesota 55455, USA*

(Received 30 April 2007; published 7 September 2007)

We propose a gravitational dual of ''single-sector'' models of supersymmetry breaking which contain no messenger sector and naturally explain the scale of supersymmetry breaking and the fermion mass hierarchy. In five dimensions these models can be given a simple interpretation. Inspired by flux-background solutions of type IIB supergravity, a metric background that deviates from AdS_5 in the IR breaks supersymmetry, while the fermion mass hierarchy results from the wave function overlap of bulk fermions with a UV-confined Higgs field. The first and second generation squarks and sleptons, which are localized near the IR brane, directly feel the supersymmetry breaking and obtain masses of order 10 TeV. These are interpreted as composite states of the dual 4D theory. The gauginos and third generation squarks and sleptons are elementary states that obtain soft masses of order 1 TeV at the loop level via direct gauge mediation. This particle spectrum leads to distinctive signatures at the LHC, similar to the usual gauge mediation with a neutralino NLSP that decays promptly to a gravitino LSP, but with lower event rates. Nevertheless we show that with 1–10 fb^{-1} of LHC data ''single-sector'' models can easily be detected above background and distinguished from conventional gravity and gauge mediation.

DOI: 10.1103/PhysRevD.76.055001 PACS numbers: 11.25.Wx, 11.10.Kk, 11.25.Tq, 11.25.Uv

I. INTRODUCTION

With the advent of reliable techniques to study dynamical supersymmetry breaking (DSB) [1] in the mid-1990's, gauge mediation[1] flourished as an alternative to its elder sibling, supergravity mediation. Gauge mediation solves the flavor problems of supergravity mediation [3], due to universality at a relatively low scale. At the same time, several proposals [4–6] were made to combine the nonperturbative dynamics that broke supersymmetry (SUSY) with a modicum of compositeness in the standard model sector of the theory. These models were closely related to ideas of minimal supersymmetric standard model (MSSM)-compositeness [7]. As in older non-SUSY models [8], light fermion masses could be explained on dimensional grounds. On the other hand, the scalar partners of these light fermions obtained masses much larger than the electroweak scale, because they coupled strongly to the DSB sector and were not protected by chiral symmetries. In the examples that were constructed during this period, the quantitative details of the multi-TeV-scale nonperturbative dynamics were ''incalculable,'' signifying qualitative but not especially quantitative predictions.

Recently, gauge/gravity duality ideas based on the anti-de Sitter/conformal field theory (AdS/CFT) correspondence in type IIB string theory [9] have been used to give a four-dimensional (4D) holographic description for models in a warped extra dimension [10]. This has led to the remarkable result that strongly coupled 4D gauge dynamics can be modeled with a five-dimensional (5D), weakly coupled gravitational theory. In this approach, classical field theory computations are able to capture the dominant effects of the strongly coupled 4D theory. For example, the Randall-Sundrum model [11] can be given a purely holographic interpretation as a 4D composite Higgs model. The warp factor is used to obtain a low symmetry-breaking scale which is then identified as the dynamical electroweak symmetry-breaking scale. In fact more recent composite Higgs models consistent with all electroweak precision tests have been constructed primarily motivated from the gravity side [12]. Ideas from AdS/CFT have even been applied to QCD, where the chiral symmetry-breaking scale is related to the warp factor [13]. Similarly warped extra dimension models have been used to break SUSY [14], where the warp factor is now used to generate a low SUSY-breaking scale which is then identified as a DSB scale. In these models boundary conditions were used to break SUSY. In the present work, we pursue this idea of relating the warp factor with a dynamically generated scale in the context of realistic, strongly coupled 4D SUSY gauge theories, softly broken by the effects of DSB. A simple 5D gravitational dual will be described that will allow previously incalculable particle mass spectra to be calculated.

A key insight is gained from recent developments in string/M theory and its effective supergravity descriptions. We note that the realizations of the AdS/CFT correspondence that are on a firm theoretical footing arise in just this context. Whereas the original correspondence was formulated in models with maximal SUSY [9], it has been known for some time now how to construct rigorous gauge/gravity

*gabella@cern.ch
†tgher@physics.umn.edu
‡giedt@physics.umn.edu

[1]For a review of gauge mediation, and references to the original articles, see [2].

dual systems with far less SUSY [15,16]. In particular, the Klebanov-Strassler solution [16] preserves $\mathcal{N} = 1$ SUSY in the 4D gauge theory. In recent work [17], the realization of bulk scalar modes was studied in this type IIB supergravity context, and related to scalars that would appear in AdS_5 phenomenological models. However, for realistic models, SUSY must be spontaneously broken and it is natural to ask whether there are non-SUSY supergravity backgrounds that might be useful for this purpose.

In fact there exist deformations of the Klebanov-Strassler background that softly break all of the supersymmetry in the infrared (IR) of the 4D theory [18,19]. It will be shown that when the ten-dimensional (10D) supergravity theory is reduced to five dimensions, the background geometry is a deformation of AdS_5, with the modification growing stronger as one moves further into the AdS throat—corresponding to SUSY-breaking near the ''IR brane'' of phenomenological models. Consequently we will use the non-SUSY background of [19] as a starting point to construct a string-inspired model with realistic phenomenology. As in the Randall-Sundrum model [11] we will introduce both a ''UV brane'' and an ''IR brane,'' and then consider bulk fields [20] by embedding the MSSM into a slice of the deformed AdS_5, with all but the Higgs fields propagating in the bulk. At low energies, the theory is described by the MSSM with SUSY-breaking soft terms that are determined by the deformed AdS_5 geometry; since the deformation is determined by a single parameter, the model is quite economical. However the deformed geometry only gives sizable soft masses to scalar fields localized near the IR brane. For the remaining sparticles we show that soft masses of the requisite scale are generated radiatively.

In particular since the gaugino masses arise at one loop in the 4D description, they must have a tree-level interpretation in the 5D theory. However, the naive action in the deformed background has a $U(1)_R$ symmetry that protects the gauginos from acquiring a mass. As we show, the tree-level mass arises from an additional contribution to the gaugino action due to the nontrivial, $U(1)_R$-violating flux background in the underlying type IIB supergravity.

The dual 4D theory that we obtain is remarkably similar to a purely 4D ''single-sector'' model constructed in Ref. [4]. We determine the crucial ratio F/M that encodes the messenger dynamics by comparing scalar masses of composite states to the results in Ref. [4]. The ratio F/M then determines the perturbative corrections that provide soft terms for all fields localized near or at the UV brane. Exploiting well-known results in gauge mediation, we find that the Higgs fields obtain the necessary soft masses from this effect, rendering electroweak symmetry breaking viable.

Consequently the particle spectrum in our model has very distinctive features and a generic spectrum is shown in Fig. 1. The first and second generation of scalar partners

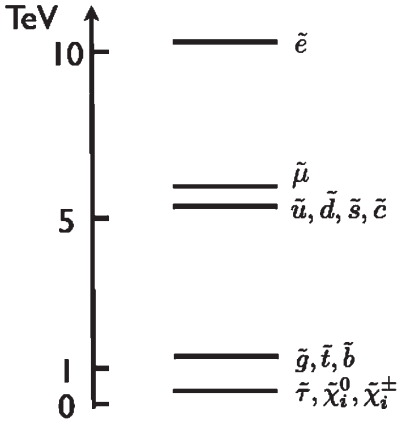

FIG. 1. The generic mass spectrum of the 5D gravity model showing the heavy first and second generation scalars and lighter third generation scalars, gluinos, neutralinos, and charginos. The LSP is the gravitino (not shown).

are very heavy. These large masses do not destabilize the Higgs mass via radiative corrections because of (1) small Yukawa couplings and (2) degeneracies at the messenger scale that prevent large one-loop hypercharge Fayet-Iliopoulos (FI) terms.[2] As will be discussed, these degeneracies are also necessary in order to satisfy flavor changing neutral current (FCNC) constraints. This spectrum is similar to that considered in Refs. [21,22] and is also reminiscent of the ''more minimal'' supersymmetric standard model [6], for which heavy first two generation scalar fields were considered to ameliorate flavor problems. The LSP is the gravitino, which means that in our model the lightest neutralino, $\tilde{\chi}_1^0$, is the NLSP. Because the messenger scale is relatively low, the decay length of $\tilde{\chi}_1^0$ is less than 1 mm. This leads to a $2\gamma + \not{E}_T$ (two hard photons and missing transverse energy) signal at the LHC. Although the event rate is reduced ($\sim 50\%$) compared to conventional gauge-mediated SUSY breaking (GMSB) due to the heavy first and second generation squarks and sleptons being inaccessible at the LHC, we show that this signal can easily be seen with 1–10 fb^{-1} integrated luminosity.

The plan for the rest of the paper is as follows: In Sec. II we present the phenomenological model from the 5D point of view and show how a natural supersymmetry-breaking scale and a fermion mass hierarchy can be simply explained by a warped extra dimension. In Sec. III we describe the dual 4D holographic interpretation of our model and its relation to 4D single-sector models. We also discuss gauge-mediated contributions to soft masses and address important phenomenological constraints from FCNC's and naturalness. In Sec. IV we discuss in detail the LHC $2\gamma + \not{E}_T$ signal of our model. We compare to rates in conven-

[2]Here it is important that the messenger scale M in our model is $\mathcal{O}(100)$ TeV, so that splittings that would disturb the degeneracies are not introduced under renormalization group evolution to the electroweak scale.

tional GMSB, and illustrate how simple cuts allow for the removal of virtually all standard model (SM) background. Finally, in the appendices we present details of bulk scalar fields, fermions, and Yukawa interactions in the deformed warped geometry as well as show how our 5D model is inspired from the 10D type IIB supergravity solution of [19].

II. THE 5D GRAVITY MODEL

We begin by defining our model using a geometrical 5D framework. In this way a naturally small scale of supersymmetry breaking with fermion mass hierarchies will be manifest. This leads to a characteristic superparticle mass spectrum with features that depend only on the broad properties of the underlying geometry. However the advantage of the 5D model is that the particle mass spectrum can be reliably calculated, and we will also explicitly present a particular mass spectrum of our 5D model to illustrate this calculational ability.

A. Deformed AdS_5

In order to break supersymmetry we will consider an effective 5D model that is motivated from a 10D type IIB supergravity solution [19], obtained by perturbing the well-known Klebanov-Strassler supersymmetric background [16], using techniques developed in [18]. In Appendix D, we describe in detail how the effective deformed nonsupersymmetric 5D background metric is obtained from a dimensional reduction of the 10D metric.[3] The resulting 5D geometry will be parametrized as:

$$ds^2 = A^2(z)(-dt^2 + d\vec{x}^2 + dz^2),$$
$$A^2(z) = \frac{1}{(kz)^2}\left[1 - \epsilon\left(\frac{z}{z_1}\right)^4\right], \tag{2.1}$$

where k is the AdS curvature scale, and $z_0 \leq z \leq z_1$ with z_0, z_1 the positions of the UV and IR branes, respectively. The parameter ϵ is related to variables in the original 10D solution (see Appendix D), although for our phenomenological purposes we only need assume it to be an arbitrary but small, positive parameter. The $\epsilon \to 0$ limit is just a slice of AdS_5, which is the 5D background setup used in the Randall-Sundrum model [11].

It is clear that the deformation of AdS_5 dominates in the IR, where z is the largest. Physical arguments and the fact that this is meant to be a small perturbation with SUSY breaking far below the AdS curvature scale $k \sim m_P$, where m_P is the (reduced) Planck scale, requires that

$$\epsilon < 1, \qquad kz_1 \lesssim \frac{m_P}{\text{TeV}} \simeq 10^{15}. \tag{2.2}$$

The actual value of the IR scale z_1^{-1} will be determined later by satisfying constraints from FCNC's and naturalness.

[3]The flux background is also deformed, and is relevant to the gaugino masses, as will be discussed.

B. MSSM in the bulk

Next we introduce the MSSM field content into the bulk with metric (2.1). In the supersymmetric limit ($\epsilon \to 0$) these 5D fields propagate in a slice of AdS and satisfy nontrivial boundary conditions [20]. Upon compactification to four dimensions, the massless zero modes of the Kaluza-Klein towers are identified with the 4D MSSM fields. Unlike in the Randall-Sundrum model, the warp factor is used to set the scale of supersymmetry breaking and is parametrized by the deformation of the AdS metric (2.1). Consequently the Higgs fields need not be localized on the IR brane and in fact we assume them to be confined on the UV brane where their masses are protected by supersymmetry. Instead the IR brane is the source of supersymmetry breaking in our model.

Furthermore, the extra dimension is used to naturally generate small Yukawa couplings for the massless fermions by wave function overlap with the UV-confined Higgs field. In particular this means that the first two fermion generations are localized predominantly near the IR brane, while the third generation fermions are nearer to the UV brane. In this way the warped extra dimension not only helps to explain the scale of supersymmetry breaking but also the fermion mass hierarchies.[4]

C. Fermion masses

Let us first consider the SM fermions. As shown in Appendix B, each SM fermion is embedded into its own 5D field. The zero mode profile for each fermion i is given by

$$f_i(z) \propto z^{1/2-c_i}, \tag{2.3}$$

where the exponent depends on a bulk mass parameter c_i. For $c_i > 1/2$ ($c_i < 1/2$) the zero mode is localized near the UV (IR) brane. The wave function overlap of the fermion zero modes with the UV-confined Higgs fields $z_* = z_0 = 1/k$, using the expression (C3) in Appendix C, leads to the 4D Yukawa couplings

$$Y_\psi = Y_\psi^{5D} k \sqrt{\frac{1/2 - c_L}{(kz_1)^{1-2c_L} - 1}} \sqrt{\frac{1/2 + c_R}{(kz_1)^{1+2c_R} - 1}}. \tag{2.4}$$

[4]A Higgs localized on the IR brane can also be considered. However, the UV-localized scalar superpartners of the first two generations only feel gauge mediation. For them to obtain sufficiently large soft masses, the scale of the IR brane must be $\mathcal{O}(100)$ TeV. This will also be the scale of the stop mass, since it is IR localized in this scenario. Such a large stop mass would clearly destabilize the Higgs mass through its $\mathcal{O}(1)$ Yukawa coupling. Nevertheless, these problems are not insurmountable, but would require additional assumptions on the model.

TABLE I. Standard model $\overline{\text{MS}}$ running fermion masses at the scale m_Z, as determined by Softsusy [23]. Also shown are the corresponding c values and 5D Yukawa couplings (in units of k) for the case of UV Higgses and $\tan\beta = 10$.

	$\bar{m}(m_Z)$	c_L	$-c_R$	Y^{5D}		$\bar{m}(m_Z)$	c_L	$-c_R$	Y^{5D}		$\bar{m}(m_Z)$	c_L	$-c_R$	Y^{5D}
e	0.503 MeV	0.350	0.350	1	d	3.9 MeV	0.456	0.456	0.059	u	1.7 MeV	0.456	0.456	0.0025
μ	103.9 MeV	0.467	0.467	1	s	67.6 MeV	0.456	0.456	1	c	0.58 GeV	0.456	0.456	0.849
τ	1.75 GeV	0.601	0.601	1	b	2.9 GeV	0.69	0.648	1	t	166 GeV	0.69	5.341	1

This expression is used to solve for the c parameters using the values of the 4D Yukawa couplings and assuming $10^{-3} \lesssim Y^{5D}_{\psi} k \lesssim 1$. (It will be seen below that it is necessary to allow a small hierarchy here, in order to avoid FCNC's from the squarks. Essentially, the c's must be degenerate among first and second generation quarks in order for the corresponding squarks to be degenerate.) The results are listed in Table I.[5]

Indeed it is seen from these values that the lighter generations are closer to the IR brane while the third generation is UV localized. Since each SM fermion is contained in a chiral supermultiplet, the corresponding scalar superpartner will be localized at the same place in the supersymmetric limit. In the deformed case, the scalar localization is qualitatively unchanged. This is because the profile is only modified in the IR, where the deformation is noticeable.

In the supersymmetry-breaking background (2.1) it is shown in Appendix B that the zero modes of bulk fermions are not lifted. The SM fermions are protected by a chiral symmetry and the gauginos by a $U(1)_R$ symmetry. These symmetries are both respected by the metric (2.1). Massless gauginos are, of course, phenomenologically unacceptable. In Appendix D 2 we take into account R-symmetry breaking that arises from the nontrivial flux background that is associated with the metric (2.1), in the type IIB solution [19]. The results that we obtain accord well with the radiatively generated gaugino mass that is evident in the 4D dual gauge theory.

D. Scalar masses

Supersymmetry is broken in the bulk by the IR deformation (2.1) of the AdS metric. The squarks and sleptons will obtain masses that depend on their localization in the bulk. However, as mentioned above, the requirement of obtaining hierarchical Yukawa couplings fixes the localization of the corresponding scalar superpartners. In this way the scalar superpartner masses are in fact related to the fermion mass spectrum.

As reviewed in Appendix A, the zero mode profile of a bulk scalar field is given at leading order (small corrections are described in the appendix) by

$$f_i(z) \propto z^{b_i - 1}, \tag{2.5}$$

where the exponent depends on a mass parameter b_i of the 5D model. By supersymmetry [20]

$$b_i = \tfrac{3}{2} - c_i, \tag{2.6}$$

which explicitly shows that once the SM fermion localization is set by c_i, the localization of the scalar zero mode is then fixed. The values $b_i < 1$ ($c_i > 1/2$) correspond to a UV-localized mode, whereas $b_i > 1$ ($c_i < 1/2$) is IR localized. Clearly it is the IR-localized scalar modes that are sensitive to the SUSY-breaking background because the deformation is only appreciable near the IR brane.

In the supersymmetry-breaking background (2.1) the scalar zero modes will obtain a mass. It is straightforward to analytically solve the equation of motion for the scalar zero modes by using a linearized (in ϵ) approximation (see Appendix A). The scalar mass squared as a function of the localization parameter b is given by

$$\tilde{m}^2 = \epsilon \frac{(1-b)(b+10)}{(kz_1)^4} \frac{(kz_1)^{1+b} - (kz_1)^{1-b}}{(kz_1)^{1-b} - (kz_1)^{b-1}} k^2 + \mathcal{O}(\epsilon^2). \tag{2.7}$$

This expression simplifies in the limit $kz_1 \gg 1$. For $b > 1$ the scalar mass simply becomes

$$\tilde{m} \approx \sqrt{\epsilon(b-1)(b+10)} z_1^{-1}, \tag{2.8}$$

while for $0 < b < 1$ we have the approximation:

$$\tilde{m} \approx \sqrt{\epsilon(1-b)(b+10)} (kz_1)^{b-1} z_1^{-1}. \tag{2.9}$$

Thus we see that for an IR-localized field ($b > 1$) the scalar mass becomes of order the IR scale z_1^{-1}, while for $b \ll 1$ and $kz_1 \sim 10^{13}$ the scalar mass is much less than a GeV. The exact expression (2.7) is plotted in Fig. 2 for three values of $z_1^{-1} = 1$, 10, and 100 TeV, and for $\epsilon = 0.05$, which exhibits the above behavior for $b > 0$. Note that as $b \to 0$ the coefficient of the ϵ term in (2.7) vanishes and the corresponding mass will be given by higher order terms. We have numerically checked that for $b < 0$ the masses are vanishingly small.

From Eq. (2.6), the values of b_i are determined by the fermion spectrum of Table I. We then apply (2.7) to obtain the squark and slepton mass spectrum of Table II. The AdS curvature scale is set by requiring $m_P^2 \simeq M_5^3/k$ where M_5 is the 5D Planck scale. Choosing $k \sim 0.1 M_5$ requires $k \simeq 10^{-3/2} m_P = 7.7 \times 10^{16}$ GeV. Consequently the model parameters are set to

[5]Running masses at the electroweak scale are chosen so as to minimize logarithmic corrections to the scalar partner masses.

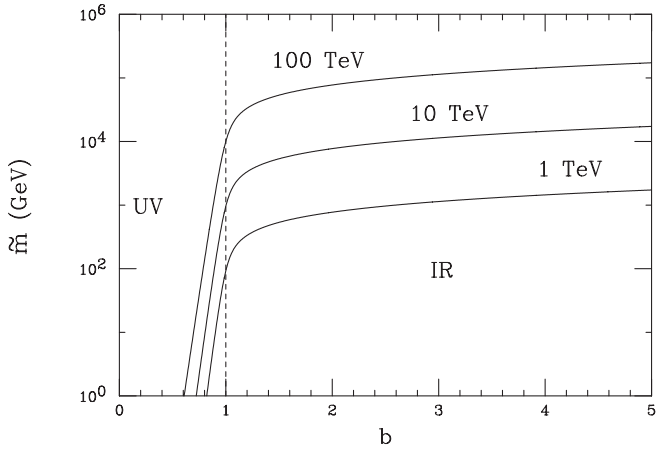

FIG. 2. The scalar mass squared (2.7) as a function of b for three values of $z_1^{-1} = 1$, 10, and 100 TeV, with $\epsilon = 0.05$. Not shown are the exponentially small values at $b \lesssim 1/2$. The values $b < 1$ correspond to a UV-localized mode, whereas $b > 1$ is IR localized.

$$\pi kR = 28.42, \qquad \epsilon = 0.05, \qquad \tan\beta = 10, \\ z_0 = k^{-1}, \qquad z_1 = (ke^{-\pi kR})^{-1} = (35\ \text{TeV})^{-1}. \tag{2.10}$$

We see that the first two generations of squarks and sleptons obtain masses of order $1/10$ to $1/20$ the Kaluza-Klein mass scale,

$$m_{\text{KK}} = \pi z_1^{-1} = 110\ \text{TeV}, \tag{2.11}$$

but the third generation masses are much smaller. As expected since the third generation fermions are near the UV brane in order to have a large overlap with the Higgs, the corresponding supersymmetry-breaking masses are phenomenologically unacceptable. However by considering the dual 4D theory we will show that there is a gauge-mediated contribution that gives rise to acceptable third generation squark and slepton masses.

III. THE 4D DUAL MODEL

According to the AdS/CFT correspondence, our 5D phenomenological model in a slice of AdS admits a 4D dual description in terms of a strongly coupled gauge theory that mixes with a fundamental sector. The supersymmetry-breaking background (2.1) is dual to DSB caused by the strongly coupled gauge theory in the IR, with a scale of order 100 TeV. The AdS/CFT dictionary identifies UV-localized fields as elementary states in the fundamental sector and IR-localized fields as bound states of the CFT. Thus our 5D phenomenological model is dual to a supersymmetric fundamental sector containing the Higgs, third generation fermions and gauge fields, while the first two generation fermions and sfermions are composite states of the dual gauge theory.

TABLE II. Soft masses, as determined by (2.7). The boundary mass parameters b are determined from (2.6), using the c-parameters given in Table I.

Sparticles	$\tilde{m}$ [TeV]	Sparticles	$\tilde{m}$ [TeV]
$\tilde{e}_{L,R}$, $\tilde{\nu}_{eL}$	10.14	$\tilde{u}_{L,R}$, $\tilde{d}_{L,R}$	5.69
$\tilde{\mu}_{L,R}$, $\tilde{\nu}_{\mu L}$	5.12	$\tilde{c}_{L,R}$, $\tilde{s}_{L,R}$	5.69
$\tilde{\tau}_{L,R}$, $\tilde{\nu}_{\tau L}$	0.468	$\tilde{b}_R$	0.149
$\tilde{t}_L$, $\tilde{b}_L$	0.051	$\tilde{t}_R$	0

A. Relation to 4D single-sector models

Interestingly, this dual model is remarkably similar to models constructed purely in four dimensions. In particular, the authors of the "single-sector" models [4,5] consider a class of theories in which DSB can be argued convincingly, and in which the first two generations of the MSSM arise as composite states ($P\bar{U}$) of a strongly coupled gauge theory. The fields $\bar{U}$ acquire large F-terms, so that the composites ($P\bar{U}$) feel the SUSY breaking directly. The first and second generation scalars get large masses, whereas the fermion composites remain massless due to chiral symmetries. Since the $\bar{U}$ fields also carry standard model charges, they communicate SUSY breaking to the rest of the MSSM through gauge mediation. The scalar masses for the first and second generation composite scalars ($P\bar{U}$) are parametrically given in Eq. (3.7) of [4] as $m_\phi^2 \sim F_{\bar{U}}^2/\bar{U}^2$. It is convenient in what follows to use the more standard notation $F_{\bar{U}} \to F$, $\bar{U} \to M$, such as appears in [2].

The messenger scale is the scale of the strong internal dynamics, corresponding to the Kaluza-Klein scale (2.11) in the gravitational dual. Taking into account the parameters chosen in (2.10), the messenger scale is thus

$$M = 110\ \text{TeV}. \tag{3.1}$$

We will assume $F \approx M$, as is common in theories where the messengers couple strongly to the DSB sector. We also require a large enough F/M in order to have a viable spectrum, and this too leads to $F \approx M$. In particular, we choose

$$F/M = 90\ \text{TeV}. \tag{3.2}$$

We note that the larger scalar masses in Table II are somewhat lower than this scale. This can be explained by the fact that the localization of the fields is such that they are in fact a mixture of composite and elementary modes. For instance, $\tilde{e}$ has $b = 1.15$, which as can be seen from Fig. 2 is just to the IR side of the dashed line that separates the two localization regimes.

The other ingredient that is needed to compute the effects of gauge mediation is the number of messengers, N_m. In practice we set $N_m = 2$, since this gives rise to an attractive LHC phenomenology and satisfies the experimental constraints that will be discussed below. We note that the $B\mu$ term and A terms are generated radiatively,

with the boundary condition that they vanish at the messenger scale (3.1). This is fairly constraining and significantly influences the model parameters. In particular, we have adjusted the model to obtain viable electroweak symmetry breaking and the lightest Higgs mass.

B. Hypercharge FI term constraints

It is important that a large FI term for hypercharge is not generated when the heavy first and second generation scalar fields are integrated out [6,21]. This amounts to imposing the constraint

$$\mathrm{Tr}\, Y\tilde{m}^2 = 0, \tag{3.3}$$

at the messenger scale. For the leptons, this is not an issue, because we can have left-right degeneracy for each generation separately, and $\mathrm{Tr}Y = 0$ for $L_i + e_i^c$, $i = 1, 2, 3$. However for the squarks, the left-right degeneracy would be broken if all the hierarchies in the 4D Yukawa couplings were generated from bulk profiles. We resolve this potential difficulty by imposing degenerate c's for the squarks of the first two generations, Q_i, u_i^c, d_i^c, $i = 1, 2$. The absence of a one-loop hypercharge FI term then follows from $\mathrm{Tr}Y = 0$ for each generation of Q_i, u_i^c, d_i^c,. The alternative is to fine-tune the left-right splitting such that

$$\tilde{m}^2_{Q_i} - 2\tilde{m}^2_{u_i^c} + \tilde{m}^2_{d_i^c} = 0, \tag{3.4}$$

where $i = 1, 2$. However, as we next discuss, FCNC constraints provide another compelling reason to impose degeneracy amongst the c's, which is what we will do in all that follows.

C. FCNC's

With all diagonal components of the 5D Yukawa couplings of order one, the soft mass matrices $\tilde{m}^2_{ij}$ that will arise from the 5D calculation are of a diagonal, nondegenerate form. Nondegenerate squarks are very dangerous, and for this reason we keep the first two generation squarks degenerate by allowing the hierarchy among 5D Yukawa couplings shown in Table I. It is interesting that the small hierarchy, m_c/m_u, in 5D Yukawa couplings mimics that which occurs in the "meson" single-sector models, where additional dynamics at a high scale was assumed to generate the necessary ratios. In addition to 1-2 mixing constraints, the generation 1-3 and 2-3 mixing cannot be too large. Since the corresponding splittings among the scalars is determined by the ratio of the Kaluza-Klein scale πz_1^{-1} to the gauge mediation scale $\alpha/(4\pi)F/M$, the IR scale z_1^{-1} cannot be too large. Note however that the wave function overlap in our model still solves the big fermion mass hierarchies, such as m_t/m_e. In Table III we compare a representative example of our model to experimental constraints, where the latter are extracted from the recent results of Ciuchini *et al.* [24]. To obtain the mixing parameters in the super-Cabibbo-Kobayashi-Maskawa (CKM) basis, it is necessary to make some assumptions regarding the quark Yukawa couplings. The assumption that reproduces the CKM matrix and leads to tree-level mixing in the down sector is[6]:

TABLE III. Comparison of our model to experimental bounds on down-type squark mixing parameters, in a standard notation. The 1-3 mixings are constrained by Δm_B and β measurements, whereas the 2-3 mixings are constrained by $b \to sX$ and Δm_{B_s} measurements. It can be seen that the latter are the most constraining.

$\lvert\delta^d\rvert$	Model	95% CL
12/LL	2.1×10^{-4}	1.4×10^{-2}
12/RR	2.1×10^{-4}	9.0×10^{-3}
12/LR	8.5×10^{-12}	9.0×10^{-5}
12/RL	4.9×10^{-13}	9.0×10^{-5}
13/LL	2.2×10^{-2}	9.0×10^{-2}
13/RR	2.1×10^{-2}	7.0×10^{-2}
13/LR	3.6×10^{-8}	1.7×10^{-2}
13/RL	5.1×10^{-11}	1.7×10^{-2}
23/LL	1.6×10^{-1}	1.6×10^{-1}
23/RR	1.6×10^{-1}	2.2×10^{-1}
23/LR	2.6×10^{-7}	4.5×10^{-3}
23/RL	6.4×10^{-9}	6.0×10^{-3}

$$Y^d = VD^dV^T, \tag{3.5}$$

where V is the CKM matrix and D^d is the diagonal matrix of down-type quark masses. This assumption is implemented in the "off the shelf" version Softsusy, and has been used to generate the "model" mixing parameters $|\delta^d|$ that are shown in Table III. Our example model has been adjusted to sit just at the edge of the exclusion bound in the most constraining channel, $b \to sX$.

Leptonic FCNC's, such as those yielding $\mu \to e\gamma$, can be avoided by assuming a diagonal lepton Yukawa matrix, since we do not embed the current theory in a grand unified theory (GUT) that would relate quark and lepton mixing.[7] The addition of a right-handed neutrino ν^c localized near the IR brane in our model would allow for Dirac neutrino masses from small effective 4D Yukawa couplings ($Y_\nu \lesssim 10^{-11}$), thereby avoiding problems of lepton flavor violation. This scenario is easily embedded into an $SU(5)$ GUT extension of our model.

D. Tachyonic stop/sbottom constraint

It is well known that heavy first two generation squarks and light third generation squarks can lead to a tachyonic

[6]An analogous assumption of mixing in the up sector can be made. However it leads to weaker constraints.

[7]In the case of a nondiagonal lepton Yukawa matrix, the dominant lepton flavor violating effects would come from diagrams involving sleptons and gauginos. A much smaller effect would arise from Kaluza-Klein Z-bosons, because they are quite heavy in this class of models.

mass squared for the latter under renormalization group evolution [25]. This effect significantly constrains the class of models considered here.

Consider the β-function for the third generation squark doublet mass squared, $d\tilde{m}^2_{Q_3}/dt$, where t is the logarithmic scale.[8] We denote by $\tilde{m}_{1,2}$ the mass scale of the first two generation squarks, and assume that this is much larger than the gluino mass M_3 and the third generation squark masses. The one-loop contribution to the β-function is

$$\beta^{(1)}_{\tilde{m}^2_{Q_3}} \approx -\frac{\alpha_s}{4\pi}\frac{32}{3}M_3^2, \tag{3.6}$$

leading to an increase in $\tilde{m}^2_{Q_3}$ as one flows to the IR. On the other hand at two loop one has

$$\beta^{(2)}_{\tilde{m}^2_{Q_3}} \approx \frac{\alpha_s^2}{(4\pi)^2}\frac{4\cdot 32}{3}\tilde{m}^2_{1,2}, \tag{3.7}$$

which tends to decrease $\tilde{m}^2_{Q_3}$ as one flows to the IR. For $\tilde{m}_{1,2} \gg |M_3|$, (3.7) dominates over (3.6), with the consequence that a small ($\lesssim 1$ TeV) value of $\tilde{m}^2_{Q_3}$ at the messenger scale M will be driven negative before reaching the scale $\tilde{m}_{1,2}$ where the first and second generation squarks decouple, provided $\tilde{m}_{1,2}$ is sufficiently far below M. In our model it is a good approximation that $\tilde{m}_{1,2} \approx 0.05M = \epsilon M$. This is a sufficient separation for the tachyonic mass squared to develop, in contrast to what occurs in models where $\tilde{m}_{1,2} \approx M$. Thus the necessity to have $\tilde{m}^2_{Q_3}(\mathrm{TeV}) > 0$ leads to the constraint:

$$\tilde{m}_{1,2} \lesssim 6M_3. \tag{3.8}$$

One concludes that in addition to the 1-3 and 2-3 FCNC constraints, the first two generation squarks must not be too heavy relative to the gluino, so as to avoid developing tachyonic masses for the third generation squarks.

In practice we have performed our renormalization group evolution analysis using Softsusy [23], where the one- and two-loop β-functions are implemented in full detail—including Yukawa couplings and mixing—rather than with the approximations (3.6) and (3.7). The discussion above is only meant to give a leading order explanation of the effect. Nevertheless, we find that the bound (3.8) is a good approximation to the full-fledged results.

E. The particle mass spectrum

In Table IV we show the complete soft mass spectrum using the two-loop RGE code Softsusy [23], for the values of the parameters given in (2.10), and $\mu < 0$ for the Higgsino mass parameter. Boundary conditions are imposed at the messenger scale (3.1), and the bulk soft masses of Table II are added in quadrature to the gauge mediation masses at that scale. Softsusy automates a self-consistent determination of the thresholds for the superpartner spectrum, taking into account one- and two-loop effects.

[8] In the discussion that follows we rely on the results of [26]. For the numerical checks, we use the two-loop running of Softsusy.

TABLE IV. Particle mass spectrum of the example single-sector model described in the text.

$\tilde{e}_L$, $\tilde{e}_R$, $\tilde{\nu}_{eL}$	10 160, 10 150, 10 160 GeV
$\tilde{\mu}_L$, $\tilde{\mu}_R$, $\tilde{\nu}_{\mu L}$	5145, 5130, 5145 GeV
$\tilde{d}_L$, $\tilde{d}_R$, $\tilde{u}_L$, $\tilde{u}_R$	5905, 5885, 5970, 5890 GeV
$\tilde{s}_L$, $\tilde{s}_R$, $\tilde{c}_L$, $\tilde{c}_R$	5905, 5885, 5970, 5890 GeV
$\tilde{g}$	1615 GeV
$\tilde{b}_1$, $\tilde{b}_2$, $\tilde{t}_1$, $\tilde{t}_2$	1354, 1369, 1253, 1369 GeV
$\tilde{\tau}_1$, $\tilde{\tau}_2$, $\tilde{\nu}_{\tau L}$	511, 630, 633 GeV
$\tilde{\chi}_1^\pm$, $\tilde{\chi}_2^\pm$	478, 593 GeV
$\tilde{\chi}_1^0$, $\tilde{\chi}_2^0$, $\tilde{\chi}_3^0$, $\tilde{\chi}_4^0$	288, 480, 511, 598 GeV
h^0, A^0, H^0, $H^\pm$	115, 646, 646, 651 GeV
$\tilde{G}$	2.35 eV

Note that these are only the masses for the lightest modes, which are zero modes in the AdS_5 limit. The Kaluza-Klein modes are at the $\mathcal{O}(100)$ TeV scale. The heavy first and second generation scalar masses arising from the bulk 5D calculation represent *bona fide* nonperturbative masses in the 4D dual theory that are difficult to calculate directly in the strongly coupled gauge theory.

The gravitino mass is obtained from the standard formula

$$m_{3/2} = \frac{F}{\sqrt{3}m_P} = 2.35 \text{ eV}. \tag{3.9}$$

Furthermore, because $\sqrt{F} = \mathcal{O}(100)$ TeV, this yields a decay length for $\tilde{\chi}_1^0$ that is a fraction of a millimeter. Thus the NLSP decays inside of a detector, with well-known collider signatures, as we will discuss in the next section.

IV. LHC STUDY

Here we present the results of a preliminary LHC study of the $pp \to 2\gamma + \not{E}_T$ signal in the example single-sector model we are studying, summarized in Table IV. The diphoton signal has been studied as a probe for new physics, for instance, by the experiments at Tevatron; an example is [27]. The present study was performed using PYTHIA (version 64.08) [28]. Subsequent studies using detector simulations would allow for a refinement of the results summarized here and would complement closely related LHC studies [29,30]. Nevertheless, it can be seen from the results given below that for the spectrum studied here, it is easy to remove virtually all backgrounds and have discovery with 1–10 fb^{-1} of data.

Because of R-parity, two SUSY particles are produced (except in the case of Higgs pair production) and at the end of the decay chain one has

$$2\tilde{\chi}_1^0 \to 2(\gamma + \tilde{G}), \tag{4.1}$$

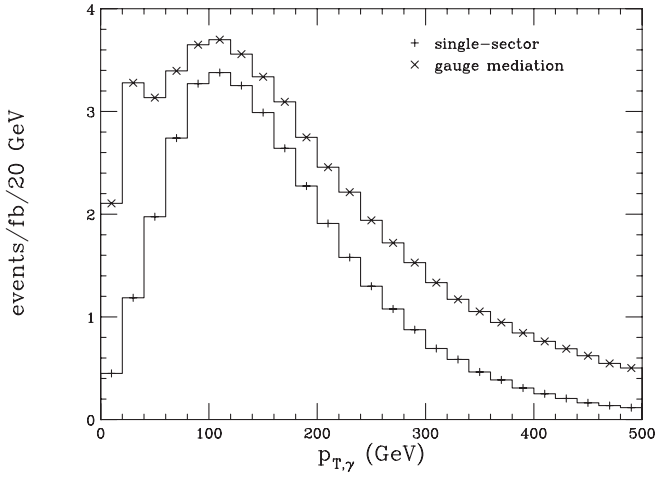

FIG. 3. The photon differential p_T distribution in our example model, compared to a comparable GMSB model, with only nominal cuts (cf. Sec. IV B 1). High p_T bins are especially useful as discriminators, and would be statistically significant with 10 fb^{-1} of data.

where $\tilde{G}$ is the gravitino. As a consequence, two very hard photons and abundant missing transverse energy ($\not{E}_T$) characterize the SUSY events. The decay length for $\tilde{\chi}_1^0$ is a fraction of a mm, so the decay occurs inside the tracking system and will be unobservable.

A. Comparison to conventional gauge mediation

As can be seen from Fig. 3, rates for the diphoton events (4.1) are reduced by a factor of ~50% relative to conventional gauge mediation with the same values of M, F/M, $\tan\beta$, number of messengers N_m, and $\mu < 0$. This is just because many sparticles in our model are beyond LHC reach, due to the large nonpertubative contribution to their masses (cf. Table II). From the scaling of the significance $S/\sqrt{B}$, we conclude that in our model ~4 times more data will be required for discovery in the diphoton channel compared to GMSB. Nevertheless, we will show below that it is easily detectable above backgrounds. Thus, we can distinguish our model from GMSB and discover it with 1 to 10 fb^{-1} of LHC data; i.e., with less than a year of "well-understood" data.

B. Signal versus background analysis

We now turn to the question of whether the diphoton signal can be seen above the standard model (SM) background at the LHC and show that it will indeed be possible.

1. Nominal cuts

We are interested in diphoton events that are reasonably clean. That is, the photon should be fairly energetic, isolated, and identifiable. Isolation cuts are imposed as follows. An inner cone of $R_{\rm in} = 0.02$ is defined, centered on the photon. The size of the cone is based on the CMS ECAL segmentation of 0.017×0.017 in $\eta \times \phi$ space. We compute the total energy $E_{\rm in}$ of all visible particles in this cone. Following [29], we define a wider cone with $R_{\rm wide} = 0.3$, again centered on the photon. Similarly we compute the total energy $E_{\rm wide}$ of all visible particles in this cone. For isolation, we require that at least 90% of the energy is contained in the inner cone. To summarize:

$$R_{\rm in} = 0.02, \qquad R_{\rm wide} = 0.3, \qquad E_{\rm in}/E_{\rm wide} \geq 0.9. \tag{4.2}$$

We also impose a kinematic cut on the photons such that they are modestly hard:

$$p_{T,\gamma} \geq 10 \text{ GeV}. \tag{4.3}$$

Finally, we require that the photons fall into the central region, where resolution and identification is optimal:

$$|\eta| \leq 2.5. \tag{4.4}$$

The solid lines in Fig. 4 show the $p_{T,\gamma}$ and $\not{E}_T$ distributions of diphoton events that pass the above cuts, obtained from the SUSY hard processes. To obtain these results, 5×10^5 events were simulated. Bin counts were subsequently re-

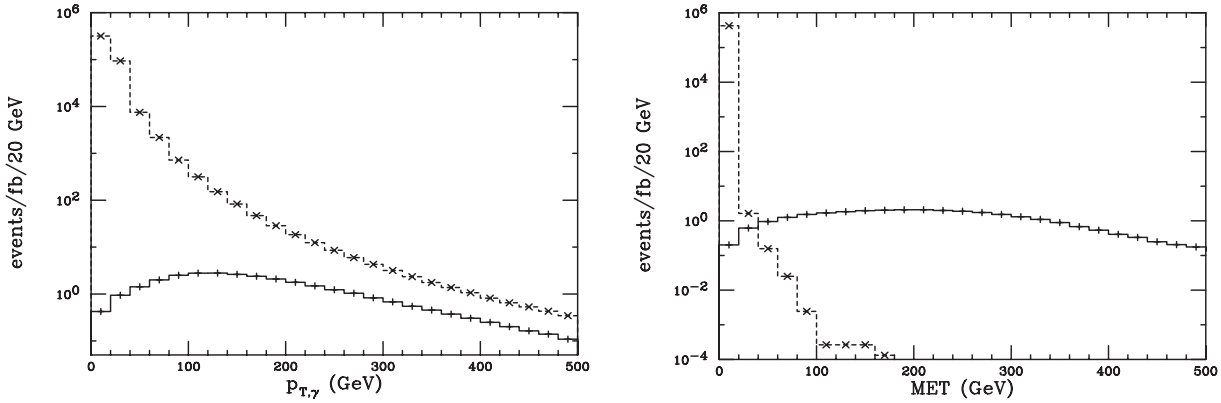

FIG. 4. Comparison of the single-sector diphoton signal (solid line) to background (dashed line) of Eq. (4.5). Here both the photon p_T and event $\not{E}_T$ distributions are shown. Only nominal cuts (cf. Sec. IV B 1) are made.

scaled to yield distributions for 1 fb^{-1} integrated luminosity. It can be seen that the diphoton events generated through the SUSY processes have a very broad $\not{E}_T$ distribution. This is largely due to the gravitinos that escape the detector. As usual, the broad $\not{E}_T$ distribution will grant us substantial leverage in removing backgrounds from the standard model processes.

2. Standard model backgrounds

The standard model produces backgrounds that would obscure the signal if only the nominal resolution cuts are made. One background is just diphoton production through standard model processes:

$$pp \to \{gg, q\bar{q}\} \to \gamma\gamma, \tag{4.5}$$

where in the intermediate step we have denoted the partons from the pp pair that contribute to the diphoton hard process. The other backgrounds involve QCD jets (j) that fake photons (mainly due to $j \sim \pi^0$):

$$pp \to \gamma j_{\text{fake}}, \qquad pp \to j_{\text{fake}} j_{\text{fake}}. \tag{4.6}$$

These backgrounds have been, for instance, discussed in [27,29]. We repeat the discussion from Sec. 4 of [29]. At the LHC, the cross sections for the three relevant standard model events are shown in Table V. The ratio of cross sections, when γ is replaced by a jet, is roughly 1:1000. The probability of a jet to fake an isolated photon is also about 1:1000. Thus each of the three channels contributes at about the same order to background. A crude estimate of the total background is therefore $3 \times (pp \to \gamma\gamma)$. We will take this approach in what follows. However, an interesting follow-on to this study would be to simulate the γj and jj events, and check to see what the effect of the background reduction cuts is on the corresponding distributions.

3. Simulation

In our background study, we simulate pp collisions at $\sqrt{s} = 14$ TeV, with the hard process selection in PYTHIA set to

$$gg, q\bar{q} \to \gamma\gamma, \tag{4.7}$$

and then show how to reduce this background relative to signal with kinematic cuts.

The background was accumulated with 4 runs of 5×10^5 events each. The runs differed by lower and upper kinematic cuts on the hard process, as implemented in PYTHIA through the variables CKIN(3) and CKIN(4), shown in Table VI. Then these were summed, weighted by the corresponding cross sections measured in each run. The reason that this was done is that the low p_T and $\not{E}_T$ standard model events would otherwise statistically overwhelm the higher bins, and one would not get a representative sample in the latter. The hard process kinematic cuts overcome this, allowing for reliable background estimates over several decades.

TABLE V. Standard model cross sections, reproduced from [29].

Channel	$\gamma\gamma$	γj	jj
Cross section	0.15 μb	0.12 mb	55 mb

TABLE VI. Arrangement of the kinematic cuts that were made for the estimation of standard model backgrounds.

Run	CKIN(3)	CKIN(4)
1	0	50
2	50	100
3	100	250
4	250	∞

The background (dashed line) is compared to signal (solid line) in Fig. 4. It can be seen from Fig. 4 that it would be challenging to detect the diphoton SUSY signal in the p_T distribution, without further cuts. (Note that the vertical axis is a logarithmic scale.) However, Fig. 4 demonstrates that the $\not{E}_T$ distribution would yield rapid discovery of "new physics" in the diphoton channel, since in all but the lowest bin the counts are far in excess of the background. Furthermore, it is clear that a $\not{E}_T$ cut will remove most of the background.

4. Background reduction cuts

We impose isolation and central region cuts as in Sec. IV B 1. As just mentioned, a $\not{E}_T$ cut will remove most of the background in the diphoton channel. Furthermore, Fig. 4 shows that the standard model diphoton events are predominantly of low p_T. Based on these results, we impose the following kinematic cuts to reduce the background:

$$p_{T,\gamma} \geq 40 \text{ GeV}, \quad \not{E}_T \geq 60 \text{ GeV}. \tag{4.8}$$

The results are shown in Fig. 5. It can be seen that backgrounds (dashed line) are orders of magnitude smaller than the signal (solid line). With 1–10 fb^{-1} of data, virtually no background events occur. We also note that the signal is hardly impacted by the cuts (4.8). This is shown in Fig. 6.

The total event rates after the cuts are shown in Table VII. We estimate the SM "2γ + fakes" rate by approximately 3 times the rate obtain from the SM diphoton events, as explained above.

C. Summary

The simple $p_{T,\gamma}$ and $\not{E}_T$ cuts (4.8) suffice to remove virtually all SM backgrounds for the $2\gamma + \not{E}_T$ signal. Discovery of the example model within the first 10 fb^{-1} of well-understood data is a certainty, and would occur during the first few years of the LHC experiment. Further studies of the jet-fake backgrounds are nevertheless war-

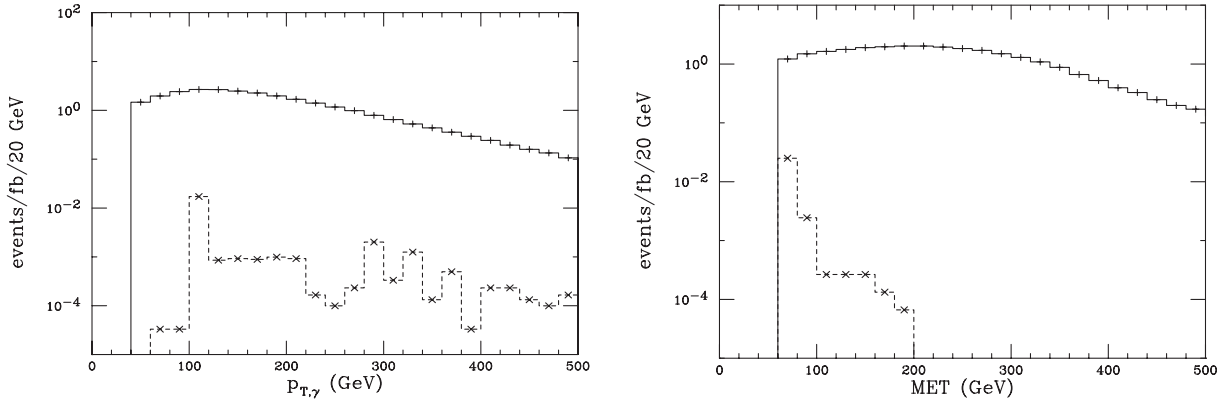

FIG. 5. Comparison of the single-sector diphoton signal (solid line) to background (dashed line) Eq. (4.5). Here both photon p_T and event $\not{E}_T$ distributions are shown. Cuts to remove background, Eq. (4.8), have been made, removing virtually all the background. It can be seen that the signal will be spectacularly visible.

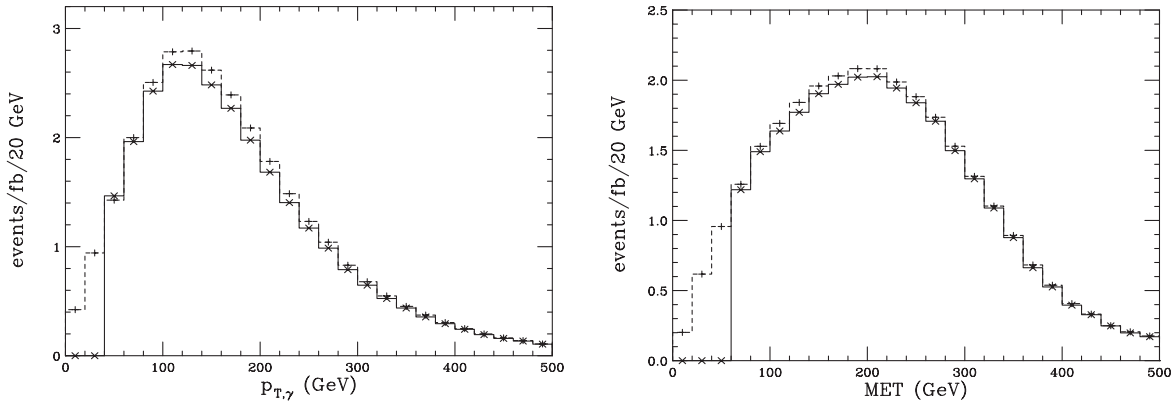

FIG. 6. Comparison of the single-sector $2\gamma + \not{E}_T$ signal before (dashed line) and after (solid line) background reduction cuts. Distributions of photon p_T and event $\not{E}_T$ are shown. It is clear that not much signal is lost from the cuts (4.8).

TABLE VII. Comparison of event rates for the $2\gamma + \not{E}_T$ channel, after cuts. Note that the standard model backgrounds are negligible, and the SUSY signal is spectacular.

Integrated luminosity	SUSY	SM 2γ	SM 2γ + fakes
1 fb^{-1}	27.6	0.0285	$\lesssim 0.1$
10 fb^{-1}	276	0.285	$\lesssim 1$

ranted, because we would like to understand the exclusion bounds for single-sector models with the $2\gamma + \not{E}_T$ signal more generally. Also, it is important to determine how $\not{E}_T$ resolution will affect our signal-to-background results, since poorly measured background events would end up in the sample after cuts. However, because the background is several orders of magnitude below the signal after our cuts are imposed, the $\not{E}_T$ resolution should not pose a difficulty for discovery of the model.

V. DISCUSSION AND CONCLUSION

We have presented a 5D dual gravity model of 4D single-sector supersymmetry-breaking models. These models naturally explain the scale of supersymmetry breaking and the fermion mass hierarchy without invoking a messenger sector. They lead to a distinctive particle spectrum consisting of heavy ($\mathcal{O}(10$ TeV)) first and second generation squark and slepton masses. The remaining sparticles are lighter ($\mathcal{O}$(TeV)) so that at low energies only the gluinos, charginos, neutralinos, and third generation squarks and sleptons will be accessible at the LHC. The LSP is the gravitino. This spectrum has been previously studied [21,22] and is reminiscent of the ''more minimal'' supersymmetric standard model [6]. The most striking signal at the LHC is from $2\gamma + \not{E}_T$, which will be easily detectable after 1–10 fb^{-1} of ''well-understood'' data is accumulated.

The dual 4D interpretation of our model is that the first two generations of fermions and bosons would be composite states of some strongly coupled gauge theory (''superglue'') that is responsible for both the scale of supersymmetry breaking via dimensional transmutation and the fermion mass hierarchy via large anomalous dimensions for fermionic operators in the gauge theory. The remaining particles are elementary fields that couple weakly to the composite supersymmetry-breaking sector.

This holographic interpretation is qualitatively identical (i.e., the "big picture" is just Fig. 1) to single-sector models that were explicitly constructed in four dimensions [4,5]. Our 5D model not only has a calculational advantage over 4D strongly coupled gauge theories, where at best only naive dimensional analysis estimates are possible, but also uses the AdS/CFT correspondence to identify the ratio of the Planck scale to the scale of supersymmetry breaking with the warp factor and the fermion mass hierarchy as arising from wave function overlap in the bulk.

While we have presented an alternative 5D interpretation of 4D models of dynamical supersymmetry breaking, further questions remain that would be interesting to explore. In particular our 5D model was motivated by type IIB supergravity solutions in ten dimensions which are described by nonsupersymmetric backgrounds that admit a dual 4D description. However these explicit supergravity solutions do not contain the MSSM particle content and therefore the MSSM fields were introduced by hand in our effective 5D gravity description. An interesting question to address is how in detail the MSSM content could in fact be obtained in the bulk from probe D7 branes [17] with the requisite values of the c parameters [31]. Once the mathematical techniques for this part of the theory are fully worked out, the field content of the dual 4D description would then be known, leading to completely defined and fully calculable models.

Our phenomenological model does not solve the little hierarchy problem or mu problem associated with the supersymmetric Higgs sector. This is not surprising since the fifth dimension does not affect this sector at tree level and we inherit the problem from the MSSM. However proposed solutions such as including a gauge singlet field in nonminimal versions of the MSSM could be straightforwardly added to our 5D scenario. In addition the fermion sector could easily be extended to include neutrino masses via the addition of a right-handed neutrino ν^c. A seesaw mechanism is naturally implemented by localizing ν^c on the UV brane or alternatively, Dirac neutrinos could be obtained from the localization of ν^c quite near the IR brane, as discussed in Sec. III C. Furthermore it would be interesting to embed our scenario into a grand unified theory. Extra dimensions have been extremely useful in providing novel ways to break gauge symmetries and such mechanisms could be implemented in our scenario. This question will also be relevant for gauge coupling unification which is essentially the same as in the MSSM provided the "preons" of the strongly coupled gauge theory arise in complete SU(5) multiplets. Nevertheless all these issues deserve further study.

Our scenario also has interesting consequences for cosmology and, in particular, dark matter. The $\tilde{\chi}_1^0$ NLSP will remain in thermal equilibrium until its mass scale is reached, with an approximate decoupling temperature $T_d \sim m_{\tilde{\chi}_1^0}/20 \approx 15$ GeV. Because of the submillimeter decay length, the neutralino density converts to gravitino LSP's immediately. In the class of models considered here the gravitino mass is $\mathcal{O}(1)$ eV, so they will be relativistic down to the temperature of galaxy formation $T_g \sim 1$ eV. Their relic abundance is therefore reduced by a factor $T_g/T_d \sim 10^{-10}$, so small as to have no effect on large-scale structure. This is to say, they are entirely harmless from an astrophysical standpoint. On the other hand, neither the NLSP nor the LSP can provide the needed dark matter density. It is an interesting question whether or not strongly interacting dark matter from the 100 TeV scale gauge theory could produce dark matter candidates with the necessary properties. Otherwise either axions or neutrinos could provide alternative possibilities.

In summary, we have provided a simple 5D framework in which to study single-sector 4D models of dynamical supersymmetry breaking. This string-inspired framework has the advantage of providing a mathematical tool in which to calculate the mass spectrum of the strongly coupled 4D theory and offers the hope of eventually building a complete model from the top down in string theory.

ACKNOWLEDGMENTS

J. G. thanks Keith Olive for helpful discussions on the cosmology of our model and Roger Rusack for input on some of the cuts that were used, relative to the CMS detector. T. G. thanks Kaustubh Agashe, Antonio Masiero, and James Wells for useful discussions on FCNC constraints. This work was supported in part by a the Department of Energy Grant No. DE-FG02-94ER40823 at the University of Minnesota. T. G. is also supported by the Research Corporation.

APPENDIX A: SCALAR FIELDS

To represent the squarks and sleptons in the bulk we first consider a complex scalar field $\Phi(x^\mu, z)$ in a slice of AdS_5 [20]. The 5D action in the background metric (2.1) reads

$$S_\Phi = \int d^4x dz \sqrt{-g}(\partial_M \Phi^* \partial^M \Phi + M_\Phi^2 \Phi^* \Phi), \qquad \text{(A1)}$$

where $g = \det g_{\mu\nu}$. The bulk mass parameter M_Φ^2 is given by

$$M_\Phi^2 \equiv ak^2 + 2bk^2 z[\delta(z - z_0) - \delta(z - z_1)], \qquad \text{(A2)}$$

where a and b are dimensionless parameters. The equation of motion

$$\partial_\mu \partial^\mu \Phi + A^{-3}\partial_5(A^3 \partial^5 \Phi) - ak^2 A^2 \Phi = 0, \qquad \text{(A3)}$$

is solved by assuming the usual separation of variables $\Phi(x^\mu, z) = \sum_{n=0}^{\infty} \phi_n(x^\mu)\tilde{f}_n(z)$. The fields $\phi_n(x^\mu)$ are the 4D Kaluza-Klein modes with profiles $\tilde{f}_n(z)$ along the extra dimension. A massless zero mode is obtained in the supersymmetric limit $\epsilon \to 0$ by imposing a modified Neumann boundary condition $(\tilde{f}_n' - bk^2 z A^2 \tilde{f}_n)|_{z_0, z_1} = 0$, and a tun-

ing, $b = 2 \pm \sqrt{4+a}$, between the bulk and boundary mass parameters. This leads to the massless mode

$$f_0(z) = \frac{1}{N}(kz)^{b-1}, \tag{A4}$$

where $N = \sqrt{(e^{2(b-1)\pi kR} - 1)/(k(b-1))}$ is a normalization constant. Note that in (A4) we have written the profile with respect to a flat metric ($f_0 = (kz)^{-1}\tilde{f}_0$) to make manifest the localization properties. Therefore for bulk masses satisfying the Breitenlohner-Freedman bound $a \geq -4$ [32], we have $-\infty < b < \infty$, and the scalar zero mode (A4) can be localized anywhere in the bulk.

In the case of the deformed AdS_5 background (2.1) with $\epsilon \neq 0$ the zero mode properties will change. Restricting to $\epsilon \ll 1$, the solution for the zero mode profile can be written as a perturbation series up to first order[9]:

$$\tilde{f}_0(z) = \tilde{f}_0^{(0)} + \epsilon \tilde{f}_0^{(1)} + \mathcal{O}(\epsilon^2), \tag{A5}$$

and accordingly for the zero mode mass squared

$$(\tilde{m}_0)^2 = (\tilde{m}_0^{(0)})^2 + \epsilon(\tilde{m}_0^{(1)})^2 + \mathcal{O}(\epsilon^2). \tag{A6}$$

The zeroth order of course corresponds to the previous solution: $\tilde{f}_0^{(0)} = (kz)^b/N$ with $\tilde{m}_0^{(0)} = 0$. Dropping all superscript indices, the equation of motion for the $\tilde{f}_0^{(1)}$ term of the zero mode profile (A5) reads

$$\tilde{f}_0'' - \frac{3}{z}\tilde{f}_0' - \frac{a}{z^2}\tilde{f}_0 = \frac{k^2}{N}\frac{(6b-a)}{(kz_1)^4}(kz)^{b+2} - \frac{\tilde{m}^2}{N}(kz)^b, \tag{A7}$$

where we have used the expansion $A'/A = -1/z - 2\epsilon z^3/z_1^4 + \mathcal{O}(\epsilon^2)$. The general solution for the profile is the combination of a homogeneous and an inhomogeneous part:

$$\tilde{f}_0 = \frac{(kz)^b}{N_1} + \frac{(kz)^{4-b}}{N_2} + \frac{(kz)^{b+2}}{8N(b-1)}\left[\frac{(b-1)(b-10)}{(kz_1)^4}(kz)^2 + 2\frac{\tilde{m}^2}{k^2}\right], \tag{A8}$$

where N_1 and N_2 are constants. By expanding the boundary conditions to first order in ϵ the constant ratio N/N_2 as a function of z and $\tilde{m}$ can be obtained. The requirement that this ratio be equal at the two boundaries leads to the desired expression for the mass of the scalar zero mode:

$$\tilde{m}_0^2 = \epsilon k^2 \frac{(b-1)(b+10)}{(kz_1)^4}\frac{e^{2\pi kRb} - 1}{e^{2\pi kR(b-1)} - 1} + \mathcal{O}(\epsilon^2). \tag{A9}$$

Note that the tuning between the bulk and boundary masses in the supersymmetric limit ($a = b^2 - 4b$) has been used since any deviation leads to higher order corrections in the masses.

[9]The underlying type IIB supergravity background is only determined to $\mathcal{O}(\epsilon)$ in any case; cf. Sec. D 1.

APPENDIX B: FERMION MASSES

A bulk fermion in a slice of AdS_5 is described by a four-component Dirac spinor $\Psi(x^\mu, z)$ whose action reads [20,33]

$$S_\Psi = -i\int d^4x dz \sqrt{-g}(\bar{\Psi} e_A^M \gamma^A D_M \Psi + M_\Psi \bar{\Psi}\Psi), \tag{B1}$$

where e_M^A is the fünfbein, and the covariant derivative $D_M = \partial_M + \omega_M$, with ω_M the spin connection. The bulk mass must be odd and is given by $M_\Psi \equiv ck\,\mathrm{sgn}(z)$ where c is a dimensionless parameter.

Massless zero modes persist in the deformed AdS_5 background. In terms of the rescaled field $\hat{\Psi} \equiv A^2\Psi$, and tangent space Dirac matrices $\{\gamma^\alpha, \gamma^\beta\} = 2\eta^{\alpha\beta}$, the equations of motion are

$$0 = (\delta_\alpha^\mu \gamma^\alpha \partial_\mu + \gamma_5 \partial_z + cA)\hat{\Psi}. \tag{B2}$$

As usual, we solve by separation of variables: $\Psi_{L,R}(x^\mu, z) = \sum_{n=0}^\infty \psi_{L,R}^n(x^\mu)\tilde{f}_{L,R}^n(z)$. For the zero modes, we set $\delta_\alpha^\mu \gamma^\alpha \partial_\mu \psi_{L,R}^0 = 0$, and obtain the solutions

$$\tilde{f}_{L,R}^0 = N_{L,R}^{-1} A^{-2}(z) \exp\left(\mp c\int_{z_0}^z dz' A(z')\right). \tag{B3}$$

Hereafter we drop the superscript and discuss only zero modes.

The background deformation has not lifted the fermion zero mode because its mass is protected by chiral symmetry. In particular, this implies that the action (B1) in the deformed background leads to massless gauginos. (However, another contribution to the gaugino action arises in the underlying type IIB supergravity background; cf. Appendix D 2.) To obtain chiral zero modes we impose a Z_2 projection in the usual manner, introducing a 5D Dirac fermion Ψ for each 4D Weyl fermion of the MSSM.

To obtain the zero mode profile, we switch to a flat 5D coordinate via

$$dy = A(z)dz \Rightarrow y = \int_{z_0}^z A(z')dz' \approx k^{-1}\left[\ln(kz) - \frac{\epsilon z^4}{8z_1^4}\right]. \tag{B4}$$

We also occasionally use the notation $\pi kR \equiv \ln(kz_1)$. The zero mode action for the 4D field $\psi_{L,R}(x)$ is then

$$\int d^4x dy A^3(y)\tilde{f}_{L,R}^2(y)\bar{\psi}_{L,R}(x)\delta_\alpha^\mu \gamma^\alpha \partial_\mu \psi_{L,R}(x), \tag{B5}$$

leading to a profile $f_{L,R} \equiv A^{3/2}\tilde{f}_{L,R}$. Thus we obtain

$$f_{L,R} = N_{L,R}^{-1} A^{-1/2}(z) \exp\left(\mp c_{L,R}\int_{z_0}^z dz' A(z')\right). \tag{B6}$$

Expanding in the small parameter ϵ we find that the profile

is virtually unchanged from what occurs in the $\epsilon \to 0$ limit:

$$f_{L,R} \approx N_{L,R}^{-1} z^{1/2 \mp c_{L,R}} \left[1 + \frac{\epsilon z^4}{4 z_1^4} \left(1 \mp \frac{1}{2} c_{L,R} \right) \right]. \quad \text{(B7)}$$

The normalization constants are[10]

$$N_{L,R}^2 = \frac{e^{2(1/2 \mp c_{L,R})\pi k R} - 1}{k(1/2 \mp c_{L,R})} [1 + \mathcal{O}(\epsilon)]. \quad \text{(B8)}$$

Again the wave function (B7) is written with respect to the flat coordinate y to make the localization properties manifest. We conclude that a left-handed fermion zero mode is UV localized for $c_L > 1/2$ and IR localized for $c_L < 1/2$, while a right-handed one is UV localized for $c_R < -1/2$ and IR localized for $c_R > -1/2$. Note that the corresponding chiral partner of the zero mode $f_{R,L} = 0$ since the Z_2 symmetry requires these fields to vanish.

APPENDIX C: YUKAWA COUPLINGS

The 4D Yukawa couplings result from a wave function overlap of the bulk SM fermions with the Higgs field [20,34]. Each SM fermion is identified with the zero mode of the corresponding 5D Dirac spinor. A Yukawa term in the 5D action with brane-localized up- and down-type Higgs fields is given by

$$\int d^4x dz \sqrt{-g} Y_\psi^{5D} \frac{H(x)}{N_H} kz \delta(z - z_*) \bar{\Psi}_R(x, z) \Psi_L(x, z), \quad \text{(C1)}$$

for a Higgs fields localized at $z = z_*$. Here, Y^{5D} is a 5D dimensionful Yukawa coupling parameter, $\Psi_{L,R}(x, z)$ is the 5D spinor that contains an $SU(2)_L$ doublet (singlet) of the MSSM as its zero mode, and $H(x)$ represents the appropriate Higgs field, H_u or H_d.

After Kaluza-Klein decomposition and integration over the extra dimension, the part concerning the zero modes reduces to

$$\int d^4x \frac{Y_\psi^{5D}}{N_H N_L N_R} (k z_*)^{-c_L + c_R} H(x) \bar{\psi}_R(x) \psi_L(x), \quad \text{(C2)}$$

from which we read the effective 4D Yukawa coupling:

$$Y_\psi = \frac{Y_\psi^{5D}}{N_H N_L N_R} (k z_*)^{-c_L + c_R}. \quad \text{(C3)}$$

The Higgs normalization constant N_H is found by requiring canonical normalization of the 4D kinetic term

$$S_H^{\text{kin}} = \int d^4x dz \sqrt{-g} \frac{kz}{N_H^2} \delta(z - z_*) g^{\mu\nu} \partial_\mu H^* \partial_\nu H, \quad \text{(C4)}$$

which implies $N_H = 1/(k z_*)$. The constants N_L and N_R are given in (B8). For UV-confined Higgs fields, $k z_* = k z_0 = 1$.

APPENDIX D: ASPECTS OF THE UNDERLYING SUPERGRAVITY

In subsection D 1, we describe how the deformed background (2.1) emerges from the non-SUSY solution given by Kuperstein and Sonnenschein (KuSo) [19]. This solution is a perturbation of the Klebanov and Strassler (KS) [16] background, governed by a small parameter δ. It is based on techniques for solving the type IIB supergravity equations of motion in the KS context that were developed in [18]. In subsection D 2, we describe how $U(1)_R$ is broken by the flux background of the KuSo solution, and how it leads to gaugino masses in the bulk.

1. The deformed background

We will be interested in the KS metric described by[11]

$$ds^2 = 2^{1/2} 3^{3/4} [e^{-5q+2Y} dx_\mu dx^\mu + \tfrac{1}{9} e^{3q-8p} (d\tau^2 + g_5^2) + \tfrac{1}{6} e^{3q+2p+y} (g_1^2 + g_2^2) + \tfrac{1}{6} e^{3q+2p-y} (g_3^2 + g_4^2)]. \quad \text{(D1)}$$

It is parametrized by

$$q, Y, p, y, \quad \text{(D2)}$$

which are all functions of the radial coordinate τ. This is related to the z coordinate through $z \sim e^{-\tau/3}$. It is important in what follows that the boundaries of our space, z_0 and z_1, are both at $\tau \gg 1$. Smaller values of τ have been integrated out and replaced by an effective IR brane, as described in [17]. For this reason, $e^{-\tau/3}$ can be treated as a small parameter in the manipulations that we now summarize.

In the KuSo background one has KS plus a small deformation. For instance,

$$q = q_0 + \delta \cdot \bar{q}, \quad \text{(D3)}$$

where δ parametrizes the deviation from the KS solution. A similar notation is introduced for the other three functions in (D2). Taking into account the various $\tau \gg 1$ asymptotic forms of the functions (D2) that are given in KuSo, we find that the metric becomes, in this limit:

[10] As usual, one integrates over $(k^2 z_1)^{-1} \le z \le z_1$, or equivalently over $-\pi R \le y \le \pi R$, to take into account the Z_2 orbifold.

[11] The five compact dimensions parametrized by the one-forms $g_1, \ldots, g_5$ are defined in [16]. They do not appear in the effective 5D metric that mimics the warped extra dimension scenario because they are averaged over in the course of dimensional reduction.

$$
\begin{aligned}
ds^2 = {} & h_0^{-1/2}[1+\delta(-5\bar{q}+2\bar{Y})]dx_\mu dx^\mu \\
& + \frac{\epsilon_{\rm KS}^{4/3}}{6K_0^2} h_0^{1/2}[1+\delta(3\bar{q}-8\bar{p})](d\tau^2+g_5^2) \\
& + \frac{\epsilon_{\rm KS}^{4/3}}{2} h_0^{1/2} K_0[1+\delta(3\bar{q}+2\bar{p}+\bar{y})]\sinh^2\frac{\tau}{2}(g_1^2+g_2^2) \\
& + \frac{\epsilon_{\rm KS}^{4/3}}{2} h_0^{1/2} K_0[1+\delta(3\bar{q}+2\bar{p}-\bar{y})]\cosh^2\frac{\tau}{2}(g_3^2+g_4^2),
\end{aligned}
\tag{D4}
$$

where h_0 and K_0 are the well-known functions that appear in the KS solution and $\epsilon_{\rm KS}$ is the parameter that describes the deformed conifold of the KS solution.

Furthermore, one has from KuSo that the leading terms in each of the functions are

$$
\begin{aligned}
\bar{q} &\approx -\tfrac{2}{5}\mu\tau e^{-4\tau/3}, \qquad & \bar{Y} &\approx \tfrac{1}{2}\mu\tau e^{-4\tau/3}, \\
\bar{p} &\approx \tfrac{3}{5}\mu\tau e^{-4\tau/3}, \qquad & \bar{y} &\approx \mu\tau e^{-\tau/3}.
\end{aligned}
\tag{D5}
$$

The parameter μ is given by

$$
\mu = 2^{10/3} 3 g_s M \ell_s^2 X \epsilon_{\rm KS}^{-8/3}, \tag{D6}
$$

where g_s is the string coupling, M is the number of fractional D3 branes, ℓ_s is the string length, and X is an integration constant in the KuSo solution that could be set to unity through a redefinition $\delta \to \delta/X$. Continuing with the expansion in powers of the small parameter $e^{-\tau/3}$, one finds

$$
\begin{aligned}
ds^2 \approx {} & \frac{2^{5/6}}{\sqrt{3\alpha\tau}} e^{2\tau/3}[1+3\delta\mu\tau e^{-4\tau/3}]dx_\mu dx^\mu \\
& + \sqrt{\frac{\alpha\tau}{3}} 2^{-5/2}\epsilon_{\rm KS}^{4/3}[1-6\delta\mu\tau e^{-4\tau/3}](d\tau^2+g_5^2) \\
& + 2^{-7/2}\sqrt{3\alpha\tau}\epsilon_{\rm KS}^{4/3}[(1+\delta\mu\tau e^{-\tau/3})(g_1^2+g_2^2) \\
& + (1-\delta\mu\tau e^{-\tau/3})(g_3^2+g_4^2)],
\end{aligned}
\tag{D7}
$$

where $\alpha = 4(g_s M \ell_s^2)^2 \epsilon_{\rm KS}^{-8/3}$.

Finally, we restrict our attention to modes that have a trivial dependence on the angular coordinates of the compact space ($T^{1,1}$ in the $\tau \gg 1$ limit), represented here by the forms g_i, $i = 1, \ldots, 5$. (Modes with a nontrivial dependence on the angular coordinates of the compact space will be excitations with mass of the order the Kaluza-Klein scale, and are therefore beyond the reach of LHC physics that we study.) With that assumption, we arrive at the effective 5D metric

$$
\begin{aligned}
ds^2 \approx {} & \frac{2^{5/6} e^{2\tau/3}}{\sqrt{3\alpha\tau}}[1+3\delta\mu\tau e^{-4\tau/3}]dx_\mu dx^\mu \\
& + \frac{\sqrt{\alpha\tau}}{4\sqrt{6}}\epsilon_{\rm KS}^{4/3}[1-6\delta\mu\tau e^{-4\tau/3}]d\tau^2.
\end{aligned}
\tag{D8}
$$

Because $\tau \sim \ln z$, the powers of τ that appear in (D8) are slowly varying relative to the powers of $e^{-\tau/3} \sim z$. On this basis we approximate the powers τ^p by a constant τ_0^p, which leads to a great simplification of the expressions that follow. The analysis in the main text is made significantly simpler by this approximation as well. Nevertheless, we capture the dominant SUSY-breaking effects of the deformed background, which is our main intent.

With this in mind, we substitute

$$
\begin{aligned}
z &= \frac{3}{2^{5/3}}\sqrt{\alpha\tau_0}\epsilon_{\rm KS}^{2/3} e^{-\tau/3}\left(1-\frac{9}{10}\delta\mu\tau_0 e^{-4\tau/3}\right), \\
\frac{\epsilon}{z_1^4} &= -\frac{2^{23/3}}{135\tau_0\alpha^2}\delta\mu\epsilon_{\rm KS}^{-8/3}, \qquad \frac{1}{k^2} = \left(\frac{27\tau_0}{8}\right)^{1/2} g_s M \ell_s^2,
\end{aligned}
\tag{D9}
$$

into Eq. (D8) where $\epsilon_{\rm KS}^{2/3}$ has dimensions of length. To $\mathcal{O}(\epsilon)$ we obtain from (D8) the deformed metric given in Eq. (2.1), as is easily verified.

2. Flux breaking of $U(1)_R$

An important issue is the origin of $U(1)_R$ breaking in the 10D supergravity description. Since the gaugino masses occur at one loop in the 4D dual gauge theory, they should be evident at tree level in the supergravity.

Fermionic terms in the supergravity action of D3-branes have been considered for instance in [35]. For the D7-branes that we expect the flavor fields to come from, the features that we now discuss should be the same, since they are understood in terms of a dimensional reduction of 10D fermions and their couplings to the closed string modes of type IIB supergravity. The important result is in Eq. (9) of [35]. There is a gaugino coupling to the type IIB supergravity 3-form $G_{(3)}$

$$
G_{ijk}\lambda\lambda + \text{H.c.}, \tag{D10}
$$

where we use a more standard notation and denote gauginos as λ. Here, G_{ijk} is the $(3,0)$ holomorphic component of $G_{(3)}$, which only has "legs" in the compact space that is orthogonal to the 5D space we are reducing to.

In the KuSo background that we study, $G_{(3)}$ is nonvanishing. Furthermore, there is a $U(1)_R \to Z(2)_R$ breaking corresponding to[12]

$$
\begin{aligned}
\int_{X_3} G_{(3)} &\approx c_1'\delta\mu e^{-\tau/3} + (c_2' + c_3'\delta\mu)e^{-\tau} \\
&\approx c_1\epsilon\frac{z}{k^2 z_1^4} + c_2 k^4 z^3 + c_3\epsilon\frac{z^3}{z_1^4},
\end{aligned}
\tag{D11}
$$

where $c_{1,2,3}$ depend at most logarithmically on z. The three-dimensional space X_3 that is integrated over is the one that describes the embedding of the D7-branes into the

[12]Further details may be found in [19,36].

compact space, which is $T^{1,1}$ in the UV. The explicit form of this embedding, which we leave arbitrary here, will determine the constants $c_{1,2,3}$. According to the AdS/CFT dictionary, the coefficients of z^3 correspond to a nonvanishing $SU(N)$ gluino condensate of the strongly coupled 4D gauge theory, and the coefficient of z corresponds to a mass for that gluino, due to SUSY breaking of the bulk. These terms provide a source of tree-level $U(1)_R$ symmetry breaking, and hence MSSM gaugino masses. Taken together with the fermionic terms of the form (D10), we thus arrive at gaugino mass terms

$$\Delta S = \int d^4x dz \sqrt{-g}\left(c_1\epsilon\frac{z}{k^2 z_1^4} + c_2 k^4 z^3 + c_3\epsilon\frac{z^3}{z_1^4}\right)\lambda_i\sigma^3_{ij}\lambda_j. \tag{D12}$$

Taking into account the gaugino profiles, the deformed metric, and the $\lambda \to g\lambda$ rescaling to obtain a canonical kinetic term (here g is the gauge coupling corresponding to λ and in the considerations here one begins in the basis where all components of a vector multiplet have $1/g^2$ as a prefactor of their kinetic terms), one finds

$$m_\lambda \approx \frac{g^2}{N_L^2}\left[\frac{c_2}{2}\left(1 - \frac{5}{24}\epsilon\right)(kz_1)^2 + \frac{c_1\epsilon}{(kz_1)^4}\ln(kz_1) + \frac{c_3\epsilon}{2(kz_1)^2}\right]. \tag{D13}$$

It can be seen that all but the first term are completely negligible. To obtain a mass that agrees with the one found at one loop in the 4D dual requires that $c_2 \approx 1/(kz_1)^3$. This presumably has to do with an embedding of the D7-branes that is supersymmetric in the $\epsilon \to 0$ limit, and is consistent with the background studied here. For instance, recall that an integral over X_3 is performed in (D11). It is a property of both the KS and KuSo backgrounds that the $\int_{S^3} G_{(3)} = 0$ for the $\tau \sim \ln z$ dependent part of $G_{(3)}$. Thus the smallness of c_2 could arise from an embedding that wraps a 3-sphere except in the immediate vicinity of the IR brane, as in [17]. It would be interesting to study this issue further, though it is beyond the scope of the present article. The main point is that there is a tree-level source of $U(1)_R$ symmetry breaking that arises from the $G_{(3)}$ flux background, and that there is a plausible 5D dual for what is found in the 4D gauge theory.

[1] For recent reviews of dynamical SUSY breaking, and references to the original literature, see for example: E. Poppitz and S. P. Trivedi, Annu. Rev. Nucl. Part. Sci. **48**, 307 (1998); Y. Shadmi and Y. Shirman, Rev. Mod. Phys. **72**, 25 (2000); K. Intriligator and N. Seiberg, arXiv:hep-ph/0702069.

[2] G. F. Giudice and R. Rattazzi, Phys. Rep. **322**, 419 (1999).

[3] L. J. Hall, V. A. Kostelecky, and S. Raby, Nucl. Phys. **B267**, 415 (1986); R. Barbieri and L. J. Hall, Phys. Lett. B **338**, 212 (1994); R. Barbieri, L. J. Hall, and A. Strumia, Nucl. Phys. **B445**, 219 (1995).

[4] N. Arkani-Hamed, M. A. Luty, and J. Terning, Phys. Rev. D **58**, 015004 (1998).

[5] M. A. Luty and J. Terning, Phys. Rev. D **62**, 075006 (2000).

[6] A. G. Cohen, D. B. Kaplan, and A. E. Nelson, Phys. Lett. B **388**, 588 (1996).

[7] A review containing many references to the older literature on this topic is: R. R. Volkas and G. C. Joshi, Phys. Rep. **159**, 303 (1988); S. Weinberg, *The Quantum Theory of Fields*, Supersymmetry Vol. III (Cambridge University Press, Cambridge, England, 2000), p. 220. More recent works on the topic are: M. J. Strassler, Phys. Lett. B **376**, 119 (1996); A. E. Nelson and M. J. Strassler, Phys. Rev. D **56**, 4226 (1997); M. A. Luty and R. N. Mohapatra, Phys. Lett. B **396**, 161 (1997); N. Okada, Prog. Theor. Phys. **99**, 635 (1998); N. Kitazawa, arXiv:hep-ph/9712223; S. L. Dubovsky, D. S. Gorbunov, and S. V. Troitsky, Phys. Lett. B **423**, 301 (1998); D. B. Kaplan, F. Lepeintre, and M. Schmaltz, Phys. Rev. D **56**, 7193 (1997).

[8] Early examples are: H. Harari, Phys. Lett. B **86**, 83 (1979); M. A. Shupe, Phys. Lett. B **86**, 87 (1979). Further references can be found in: E. Farhi and L. Susskind, Phys. Rep. **74**, 277 (1981).

[9] J. M. Maldacena, Adv. Theor. Math. Phys. **2**, 231 (1998); S. S. Gubser, I. R. Klebanov, and A. M. Polyakov, Phys. Lett. B **428**, 105 (1998); E. Witten, Adv. Theor. Math. Phys. **2**, 253 (1998).

[10] N. Arkani-Hamed, M. Porrati, and L. Randall, J. High Energy Phys. 08 (2001) 017; R. Rattazzi and A. Zaffaroni, J. High Energy Phys. 04 (2001) 021; M. Perez-Victoria, J. High Energy Phys. 05 (2001) 064.

[11] L. Randall and R. Sundrum, Phys. Rev. Lett. **83**, 3370 (1999).

[12] K. Agashe, R. Contino, and A. Pomarol, Nucl. Phys. **B719**, 165 (2005).

[13] J. Erlich, E. Katz, D. T. Son, and M. A. Stephanov, Phys. Rev. Lett. **95**, 261602 (2005); L. Da Rold and A. Pomarol, J. High Energy Phys. 01 (2006) 157; E. Katz, A. Lewandowski, and M. D. Schwartz, Phys. Rev. D **74**, 086004 (2006).

[14] T. Gherghetta and A. Pomarol, Nucl. Phys. **B602**, 3 (2001).

[15] I. R. Klebanov and E. Witten, Nucl. Phys. **B536**, 199 (1998).

[16] I. R. Klebanov and M. J. Strassler, J. High Energy Phys. 08 (2000) 052.

[17] T. Gherghetta and J. Giedt, Phys. Rev. D **74**, 066007 (2006).

[18] V. Borokhov and S. S. Gubser, J. High Energy Phys. 05

(**2003**) 034.
[19] S. Kuperstein and J. Sonnenschein, J. High Energy Phys. 02 (2004) 015.
[20] T. Gherghetta and A. Pomarol, Nucl. Phys. **B586**, 141 (2000).
[21] S. Dimopoulos and G. F. Giudice, Phys. Lett. B **357**, 573 (1995).
[22] A. Pomarol and D. Tommasini, Nucl. Phys. **B466**, 3 (1996).
[23] B. C. Allanach, Comput. Phys. Commun. **143**, 305 (2002).
[24] M. Ciuchini, A. Masiero, P. Paradisi, L. Silvestrini, S. K. Vempati, and O. Vives, arXiv:hep-ph/0702144.
[25] N. Arkani-Hamed and H. Murayama, Phys. Rev. D **56**, R6733 (1997).
[26] S. P. Martin and M. T. Vaughn, Phys. Rev. D **50**, 2282 (1994).
[27] CDF Collaboration, ''Search for anomalous diphoton plus X production,'' 2006 report at http://www-cdf.fnal.gov.
[28] T. Sjostrand, S. Mrenna, and P. Skands, J. High Energy Phys. 05 (2006) 026.
[29] F. Charles, CMS Note 1997/079.
[30] M. Kazana, G. Wrochna, and P. Zalewski, CMS Conference Report No. 1999/019.
[31] B. S. Acharya, F. Benini, and R. Valandro, arXiv:hep-th/0612192.
[32] P. Breitenlohner and D. Z. Freedman, Phys. Lett. B **115**, 197 (1982).
[33] Y. Grossman and M. Neubert, Phys. Lett. B **474**, 361 (2000).
[34] T. Gherghetta, arXiv:hep-ph/0601213.
[35] M. Grana, Phys. Rev. D **66**, 045014 (2002).
[36] A. Loewy and J. Sonnenschein, J. High Energy Phys. 08 (2001) 007.